Rail. Eng. Science (2022) 30(4):482–493
https://doi.org/10.1007/s40534-022-00274-1

System reliability evaluation of long railway subgrade slopes considering discrete instability

Wensheng Zhang[1,2,3] · Qiang Luo[1,3] · Tengfei Wang[1,3] · Qi Wang[1,3] · Liangwei Jiang[1,3] · Dehui Kong[1,3]

Received: 23 November 2021 / Revised: 28 March 2022 / Accepted: 28 March 2022 / Published online: 1 June 2022

Abstract This paper develops a dual-indicator discrete method (DDM) for evaluating the system reliability performance of long soil subgrade slopes. First, they are segmented into many slope sections using the random finite element method, to ensure each section statistically contains one potential local instability. Then, the *k*-out-of-*n* system model is used to describe the relationship between the total number of sections *n*, the acceptable number of failure sections *m*, the reliability of sections R_{sec}, and the system reliability R_{sys}. Finally, *m* and R_{sys} are jointly used to assess the system reliability performance. For cases lacking spatial data of soil properties, a simplified DDM is provided in which long subgrade slopes are segmented by the empirical value of section length and R_{sec} is substituted by that of cross-sections taken from them. The results show that (1) DDM can provide the probability that the actual number of local instabilities does not exceed a desired threshold. (2) R_{sys} decreases with increasing *n* or decreasing R_{sec}; that is, it is likely to encounter more local instabilities for longer or weaker subgrade slopes. *n* is negatively related to the horizontal scale of fluctuation of soil properties and positively related to the total length of subgrade slopes *L*. (3) When *L* is sufficiently large, there is a considerable opportunity to meet local instabilities even if R_{sec} is large enough.

Keywords Subgrade slope · Local instability · Segmentation · *k*-out-of-*n* system · System reliability · Railway engineering

1 Introduction

Soil subgrade is widely used in railway engineering worldwide, such as in the South Coast rail line in Australia [1] and the Lanzhou-Xinjiang rail line in China [2]. The instability of subgrade slopes is one of the main risk sources of railway operations due to the potential for huge social and economic impacts and even passenger casualties. For example, the Ingenheim derailment accident in France caused by a landslide due to heavy precipitation (see Fig. 1) caused 21 injuries and serious damage to vehicles [3]. Rainfall is one of the most significant triggering factors for slope failures in many regions [4]. For long subgrade slopes composed of spatial variable soils, the resisting moment of the potential local failure surface at different locations varies significantly, and it is highly likely to encounter discretely distributed local instability events along the length direction [5]. Since any local slope instability event may cause traffic disruption, the reliability assessment of subgrade slopes should be treated as a system problem. For the system reliability evaluation of subgrade slopes, the key target is to estimate the probability that the actual number of local instability events does not exceed an acceptable threshold, such as 1.

Traditionally, deterministic plane strain analyses are adopted to assess the stability level of a set of cross-sections taken from long subgrade slope via the factor of safety (*F*) [6, 7], in which characteristic values are used to represent spatially variable soil parameters. When *F* is no smaller than a predetermined value, such as 1.25, the entire subgrade slope is deemed sufficiently safe. More recently, probabilistic

✉ Qiang Luo
lqrock@swjtu.edu.cn

[1] School of Civil Engineering, Southwest Jiaotong University, Chengdu 610031, China

[2] Department of Civil and Environmental Engineering, Harbin Institute of Technology, Shenzhen 518055, China

[3] MOE Key Laboratory of High-Speed Railway Engineering, Southwest Jiaotong University, Chengdu 610031, China

Fig. 1 An example of local instability of subgrade slopes

plane strain analyses have been developed and widely used, e.g., the first-order reliability method [8–10] and the random finite element method (RFEM) [11]. The random variable or two-dimensional random field is used to describe the spatial variability of soil property, and the reliability level of cross-sections is evaluated in terms of reliability (R), probability of failure (P_f), or reliability index (β) [12]. Nevertheless, an infinite rupture surface in the length direction is assumed in the above two-dimensional analysis methods, which is not in line with reality. As soil parameters are naturally variable in three-dimensional space, the reliability of a cross-section is not representative of that of long subgrade slopes, especially when there are large fluctuations in soil properties. Previous research has shown that the reliability of three-dimensional earth slopes can be largely lower than that of a cross-section taken from them when the length is large enough, which is known as the length effect [13–15]. Thus, when the cross-sections taken from a long subgrade slope all have enough reliability, the reliability of this subgrade slope can still be very low. In other words, there may be a considerable possibility to encounter one or more local failure events. Parameters F or β only provides engineers with rough confidence that no local sliding event will occur along subgrade slopes.

Over the past decades, three-dimensional probabilistic analysis techniques have been developed to assess the reliability of long subgrade slopes, in which a three-dimensional random field is used to model spatially variable soil properties. For long slope composed of statistically homogeneous soils, using the local averaging theory and first-crossing theory, Vanmarcke [14, 15] proposed an analytical method to compute the system reliability (R_{sys}) that no local failure event will occur. The sliding mass is assumed to be a cylinder bounded by two vertical planes in Vanmarcke method. Statistically, homogeneous soil properties mean that the scale of fluctuation (SOF) and the statistics such as mean and variance are constant in earth space [16]. The SOF is an indicator of the distance within which soil property values show a strong correlation, which is defined as the area under the autocorrelation function curve [16–18]. There are various methods to estimate the value of SOF using field testing data (e.g., cone penetration testing (CPT) data), such as the method of moment, maximum-likelihood estimation, and Bayesian analysis [19]. Based on three-dimensional RFEM, Hicks and Spencer [5] developed a numerical method to calculate the R_{sys} that no local failure event will occur for long slopes consisting of statistically homogeneous soils. The RFEM is regarded as a versatile approach to predict the responses of large-scale subgrade slopes, mainly because no prior assumption concerning the location and shape of failure surfaces is required. However, it is not trivial to carry out a full three-dimensional probabilistic analysis for long earth slopes due to the immense computational expense. A VNK (Veiligheid Nederland in Kaart) method with less computational effort was proposed in the Netherlands when assessing the system reliability of dike rings [20–22]. A dike ring is divided into multiple adjacent segments within which soil properties can be regarded as statistically homogeneous, and the length of each segment ranges from 150 to 2000 m, with an average of 750 m [21–23]. The reliabilities of all segments are combined to obtain the probability that no instability event occurs in any segment, i.e., system reliability, in which the series system model is adopted. A series system means failure of any segment triggers the loss of system function [24, 25], which is applicable to flood defense since breaches in any location will cause flooding and vast losses. The abovementioned three-dimensional approaches can be classified into two categories: continuous and discrete methods. The former treats a long slope as an indivisible object, such as Vanmarcke and RFEM method. The latter treats a long slope as a discrete system composed of many components, such as VNK method. They both use one single indicator (i.e., R_{sys}) to describe the reliability level of long slopes, which provides engineers with confidence that no local instability event will occur. The occurrence probability that the number of local failure events does not surpass a tolerated quantity more than zero cannot be obtained.

To evaluate the system reliability of long continuous subgrade slopes considering multiple potential local instabilities, this work proposes a dual-indicator discrete method (DDM) easy to be employed in practice. The properties of soils are assumed to be statistically homogeneous. First, a long subgrade slope is equally divided into many adjacent sections based on the number of local instabilities predicted by RFEM. Each section statistically contains a potential instability. Then, the k-out-of-n system model is adopted to describe the relationship between the acceptable number of failure sections, the reliability of sections, and the reliability of the entire subgrade slope. Finally, two indicators named acceptable failure ratio η_{acc} and system failure probability

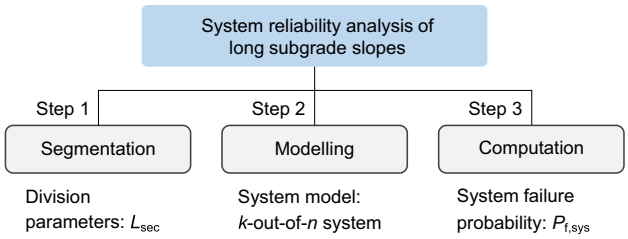

Fig. 2 Diagram of the process of DDM

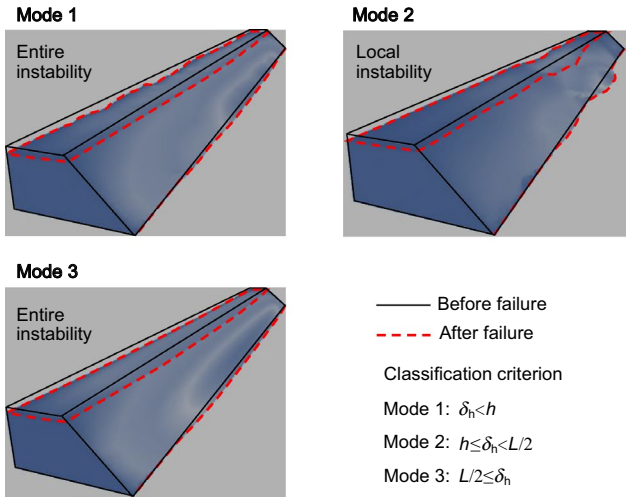

Fig. 3 Three failure modes of earth slope (after Hicks and Spencer [5])

$P_{f,sys}$ are used to describe the reliability level of subgrade slopes together. η_{acc} is the ratio of the acceptable number of local failures to the total number of sections, and $P_{f,sys}$ presents the possibility that the acceptable failure ratio is exceeded by actual failure ratios. Figure 2 presents the diagram of the process of DDM. It is noted that, for the system reliability design of new subgrade slopes, engineers usually want the probability of no local instability to be greater than a prescribed value, e.g., 95%. But for the system reliability evaluation of existing subgrade slopes, engineers need a more comprehensive understanding of the level of system safety, not just the probability of no instability, but the occurrence probability of multiple instabilities. Actually, it is not rare that multiple local failure events are encountered along a rail line in engineering practice.

The rest of this paper is organized as follows. In Sect. 2, the segmentation method of long subgrade slope is established. In Sect. 3, the k-out-of-n system is introduced to derive the expression of the system reliability of subgrade slopes. In Sect. 4, a case study is provided to illustrate the use of DDM in current engineering practice, where spatial data of soil properties is unavailable. In Sect. 5, some concluding remarks are listed.

2 Segmentation of long subgrade slope

2.1 Discrete instability modes of long subgrade slope

Using the three-dimensional RFEM, Hicks and Spencer [5] identified three modes of instability of long soil slopes composed of statistically homogeneous soils, as illustrated in Fig. 3. The analyzed long slope has an angle of 45°, a height of 5 m, and a length of 100 m. The investigation shows that the instability modes depend on the magnitude of the horizontal SOF δ_h of soil strength parameters relative to slope length L and height h, and has little relationship with the vertical SOF δ_v. In the study, δ_h ranges from 1 to 1000 m, and δ_v is fixed as 1 m. The following are general outlines of the three failure modes.

Mode 1: For $\delta_h < h$, as the δ_h is too small to allow a rupture surface to develop through semi-continuous weaker zones, the failure occurs through weak and strong zones along its entire length. This mode is analogous to a two-dimensional deterministic analysis based on mean values of soil properties.

Mode 2: For $h \le \delta_h < L/2$, the δ_h becomes large enough and local failure mass propagates much possibly through horizontal semi-continuous weaker zones. The reliability of a slope decreases with increasing L due to the increased chance of encountering a zone weak enough to trigger a failure.

Mode 3: For $L/2 \le \delta_h$, the soil presents a layered appearance and the failure extends along the length of a slope, resulting in a global failure. In this case, the failure surface develops along weak layers and appears analogous to that from a two-dimensional stochastic analysis.

According to Phoon and Kulhawy [18], El-Ramly et al. [17], and others [26, 27], the horizontal SOF of soil properties typically ranges between 10 and 100 m for various soil types. In engineering practice, the subgrade slope height mostly varies from 3 to 20 m, whereas the length could extend from several to tens of kilometers. A prominent feature of subgrade slopes is the large value of L/δ_h and L/h. Therefore, the instability mode for long subgrade slopes will theoretically be mode 2, which is in line with practical observations.

2.2 Prediction of the number of local instabilities

For short soil slopes, it is less possible to encounter many failure events owing to the lower probability of more than one weak domain existing along the length direction [13]. But, the occurrence probability rises with increasing slope length. For example, multiple local instabilities can be found

in long subgrade slopes along operating railway lines. The prediction of the number of potential local instabilities is important for the system reliability evaluation of subgrade slopes. A study by Hicks and Li [13] regarding mode 2 provides a possible way to determine the number of local instabilities for long subgrade slopes.

Using the three-dimensional RFEM, the discrete failure features of $L = 500$ m long slope composed of statistically homogeneous cohesive soils, with a height $h = 5$ m and an angle of 26.6°, were explored by Hicks and Li [13]. Four values of δ_h were utilized, namely 12, 24, 50, and 100 m, respectively. The vertical SOF was taken as a constant of 1 m since it has little effect on the discrete failure feature of long slopes [5]. The safety factor based on mean property values was fixed as 1.30. For each case of δ_h, 1000 Monte Carlo simulations for the random field of soil properties were carried out, and the number of discretely distributed local instabilities was counted. Hicks and Li [13] indicate that the number of local failures is significantly influenced by δ_h. There can be many discrete failures within the length when δ_h is small, and the number declines apparently with the increase of δ_h. Based on the number of discrete failures of 1000 Monte Carlo realizations, as shown in Fig. 4, the 95% quantile of the failure number is around $N_{95} = 9$ as $\delta_h = 12$ m, and N_{95} decreases to 6, 4, 3 as the δ_h grows up to 24, 50, and 100 m, respectively. Besides, basedon the failure feature of mode 3, the number of failure events will be 1 when $\delta_h = L/2$ and L.

Theoretically, to get the number of potential local instabilities for subgrade slopes, the full-size RFEM model can be built and analyzed. However, it is extremely difficult to apply the RFEM to all subgrade slopes encountered in practice due to the formidable computational cost. A simple yet effective way is established herein to predict the number

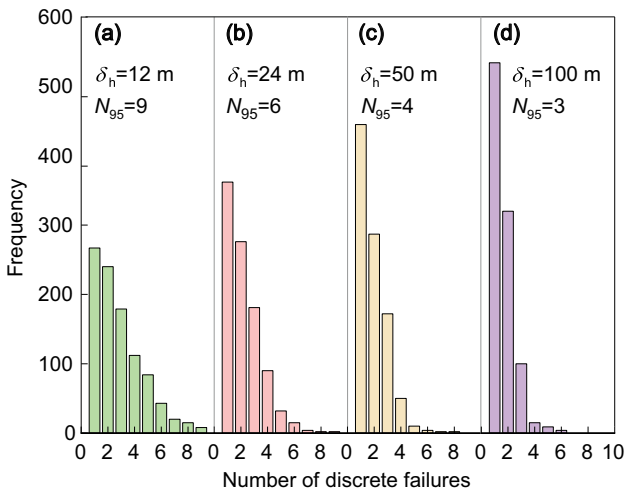

Fig. 4 The number of discrete failures at different δ_h (after Hicks and Li [13])

of discrete local instabilities for subgrade slopes with any length, based on the study of Hicks and Li [13]. As the slope with a length of 500 m is long enough to eliminate the influence of boundary conditions on the stability analysis results, the 95% quantiles in Fig. 4 could largely represent the upper bound of the number of potential local instabilities. Hence, these statistical results are seen as a benchmark to predict the number of potential failures for longer subgrade slopes. As listed in Table 1, the N_{95} for 500 m long slope is extended as the number of potential local failures per kilometer (N_{1km}) by multiplying a factor of two. Then, the total number of potential discrete local instabilities is expressed by

$$n = N_{1km} \times L, \tag{1}$$

where the total length L of subgrade slopes is in kilometers.

For illustration, providing $L = 100$ km long subgrade slope with similar geometries and soil properties to those in Hicks and Li [13], if $\delta_h = 24$ m, the n will be $12 \times 100 = 1200$. It should be noted that the values shown in Table 1 are only applicable to situations that slope geometries and soil properties are similar to the model used in the literature [13], not necessarily suitable for more general circumstances. Further research is required to examine the effect of slope geometries as well as soil properties on the number of potential local instabilities.

2.3 Segmentation of long subgrade slope

Since soil properties are statistically homogeneous in three-dimensional space, a subgrade slope with n predicted potential local instabilities is equally divided into n adjacent sections. Each section statistically contains no more than one potential local instability event, with a confidence of 95%. The stability status of arbitrary two sections would be largely independent, and the failure probabilities of any two sections are assumed to be independent in this work. In reality, the stability status of two adjacent sections may be related, and strictly speaking, this dependency should be measured and considered when analyzing the system reliability of subgrade slopes. However, this relevance is hard to be determined. In addition, based on probability theory,

Table 1 Results of numerical simulation (including data from Hicks and Li [13])

δ_h (m)	N_{95}	N_{1km}	L_{sec} (m)	l_{sli} (m)
12	9	18	55.6	13.3 ± 8.0
24	6	12	83.3	17.7 ± 9.9
50	4	8	125.0	27.4 ± 15.2
100	3	6	166.7	47.5 ± 27.3

"A ± B" stands for "mean ± standard deviation"

when the reliability of components is assumed to be independent, the results of system reliability analysis are on the conservative side. Based on the value of N_{95}, the average lengths L_{sec} of subgrade slope sections are computed and listed in Table 1. For instance, suppose the $\delta_h = 24$ m, then $L_{sec} = 500/6 = 83.3$ m. Since n is obtained according to the 95% quantile of the RFEM simulation data, L_{sec} represents a minimum length within which one potential failure event could occur in a statistical sense.

Besides, the means and standard deviations of the length of sliding masses (l_{sli}) are added in Table 1. L_{sec} is approximately four folds of the mean of l_{sli}. The ratio of L_{sec}/δ_h is negatively related to δ_h, decreasing from 4.5 to 3.5, 2.5, and 1.5 when δ_h increases from 12 to 24, 50, and 100 m, respectively.

3 System reliability evaluation of long subgrade slope

3.1 *k*-out-of-*n* model and system reliability formula

Based on the standard of ISO2394 [28], system reliability is defined as the ability of a structure with more than one structural member to fulfill specified requirements. That is, the system reliability analysis depends on the definition of a specified requirement. For a subgrade slope consisting of n sections, it is required that at least k ($0 < k \le n$) sections are normal, and accordingly, the maximum tolerated failure section is $m = n - k$ ($0 \le m < n$). This can be modeled by the k-out-of-n system [25], as shown in Fig. 5. If $m = 0$, the system is called the series system [24, 25], which is a special case of k-out-of-n system. Letting the actual number of failure sections be m_{act}, the actual failure ratio and acceptable failure ratio can be computed by $\eta_{act} = m_{act}/n$ and $\eta_{acc} = m/n$, respectively, where η_{act} and η_{acc} are normalized variables ranging from 0 to 1.

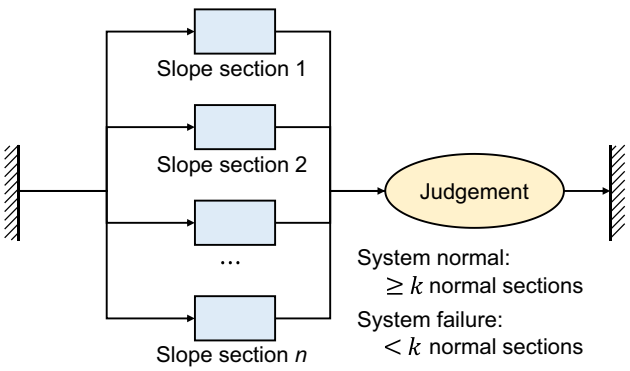

Fig. 5 Schematic of k-out-of-n system model

Then, the system normal state of subgrade slope can also be defined by $\eta_{act} \le \eta_{acc}$, and the system failure state means $\eta_{act} > \eta_{acc}$. The system reliability R_{sys} stands for the probability that $\eta_{act} \le \eta_{acc}$, and the $P_{f,sys}$ presents the probability that $\eta_{act} > \eta_{acc}$. If all sections have the same failure probability $P_{f,sec}$, the system failure probability is given by

$$P_{f,sys} = 1 - \sum_{i=0}^{m} \binom{n}{i} \left(P_{f,sec}\right)^{i} \left(1 - P_{f,sec}\right)^{n-i}, \tag{2}$$

where $\binom{n}{i} = n!/[i!(n-i)!]$ is the binomial coefficient.

In engineering practice, failure probabilities of different subgrade slope sections are generally different. To compute the system failure probability $P_{f,sys}$, all possible combinations of section statuses fulfilling the system failure state need to be considered. These combinations are referred to as system failure scenarios. The total number of system failure scenarios is given by

$$Q = \sum_{j=0}^{m} \binom{n}{j} = \binom{n}{0} + \binom{n}{1} + \cdots + \binom{n}{m}. \tag{3}$$

Let status vector $\boldsymbol{S}$ represent a specific combination of section statuses. Each element of the vector corresponds to a section with specified status, where 1 stands for the normal state and 0 stands for the failure state. The length of $\boldsymbol{S}$ equals n. For instance, if the allowable failure number is $m = 0$, the number of possible combinations is $Q = \binom{n}{0} = 1$, and the status vector will be $\boldsymbol{S}_1 = (1, 1, \ldots, 1, 1)^T$ where "T" stands for transpose. Similarly, as $m = 1$, there are $Q = \binom{n}{0} + \binom{n}{1} = n + 1$ possibilities of combinations, including $\boldsymbol{S}_1 = (1, 1, \ldots, 1, 1)^T$, $\boldsymbol{S}_2 = (1, 1, \ldots, 1, 0)^T$, etc. All above status vectors form the status matrix $\boldsymbol{\Omega}_{sce}$:

$$\boldsymbol{\Omega}_{sce} = \left(\boldsymbol{S}_1, \boldsymbol{S}_2, \cdots, \boldsymbol{S}_Q\right)_{n \times Q}. \tag{4}$$

$\boldsymbol{\Omega}_{sce}$ contains all possible combinations of section statuses satisfying system failure state, with a size of $n \times Q$. For any status vector $\boldsymbol{S}_q$ ($q = 1, 2, \ldots, Q$), the sets of subscripts of normal and failure sections are denoted by Nor_q and Fai_q, respectively. Take $\boldsymbol{S}_1$ as an example, the Nor_1 will be $\{1, 2, \ldots, n\}$ and Fai_1 will be empty. Then, the occurrence probability of the q-th system failure scenario is expressed as

$$P_{f,q} = \prod_{\text{Fai}} P_{f,sec} \prod_{\text{Nor}} \left(1 - P_{f,sec}\right). \tag{5}$$

Then, the system failure probability is the sum of $P_{f,q}$:

$$P_{f,sys} = \sum_{q=1}^{Q} P_{f,q}. \tag{6}$$

Equation (2) is a special case of Eq. (6) where all components have the same failure probability $P_{f,sec}$.

3.2 Two indicators describing system reliability

The acceptable failure ratio η_{acc} and the system failure probability $P_{f,sys}$ should be used synergistically to describe the reliability level of long subgrade slopes. Among them, η_{acc} reflects the engineers' expectations and requirements for the reliability of subgrade slopes, and $P_{f,sys}$ quantifies the possibility that η_{acc} is exceeded by the actual failure ratio η_{act}. For instance, if a $P_{f,sys} = 0.6\%$ (i.e., system reliability index $\beta_{sys} = 2.5$) is obtained when setting $\eta_{acc} = 1\%$, one has a 99.4% confidence that η_{act} is no greater than 1%.

For subgrade slopes with different degrees of failure consequence, different values of η_{acc} should be adopted. The second generation of Eurocode 7, to be published in the early 2020s [29], classifies geotechnical structures into three geotechnical categories (GC) that combine the consequence class (CC) and the geotechnical complexity class (GCC). For GC1, GC2, and GC3, the values of 1.0%, 0.5%, and 0.1% are suggested for η_{acc}, as shown in Table 2. The $\eta_{acc} = 1\%$ means that only one component is allowed to fail in every 1000 components in a *k*-out-of-*n* system. For some special structures such as monumental structures or structures that will have unbearable consequences of failing, the series system model should be utilized, i.e., $\eta_{acc} = 0$.

3.3 Factors influencing system failure probability

This section investigates the influence of the number of sections n, section failure probability $P_{f,sec}$, and the acceptable failure ratio η_{acc} on the system failure probability $P_{f,sys}$, based on Eq. (2).

3.3.1 Influence of section reliability on system failure probability

Figure 6 shows the system failure probability $P_{f,sys}$ versus section failure probability $P_{f,sec}$. A range of 3.17×10^{-5} –1.59×10^{-1} for $P_{f,sec}$ is considered, corresponding to a range of 4.0–1.0 of section reliability index β_{sec}. The total section number $n = 1000$ and the acceptable failure ratio

Table 2 Selection of acceptable failure ratio

CC	GCC/η_{acc}		
	Lower (GCC1)	Normal (GCC2)	Higher (GCC3)
CC4 (highest)	GC3/0.1%	GC3/0.1%	GC3/0.1%
CC3 (higher)	GC2/0.5%	GC3/0.1%	GC3/0.1%
CC2 (normal)	GC2/0.5%	GC2/0.5%	GC3/0.1%
CC1 (lower)	GC1/1.0%	GC2/0.5%	GC2/0.5%

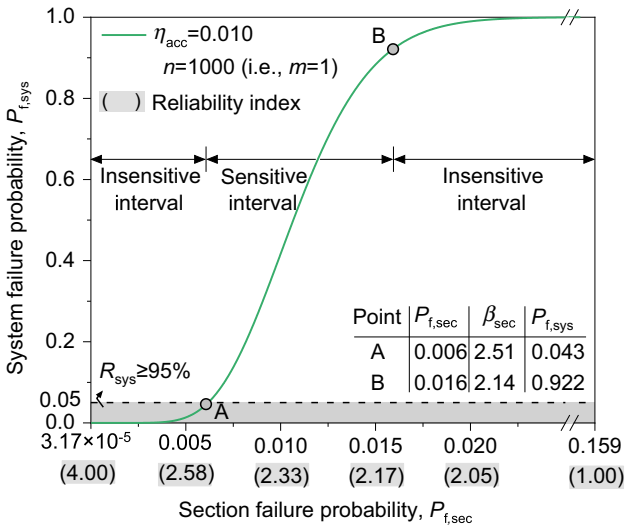

Fig. 6 $P_{f,sys}$ versus $P_{f,sec}$

$\eta_{acc} = 0.010$ are utilized for illustration ($m = n \times \eta_{acc} = 1$). In Fig. 6, $P_{f,sys}$ has an S-shaped curve and keeps rising with the increase of $P_{f,sec}$, indicating that weak components always result in poor performance of the system. $P_{f,sys}$ grows up sharply in the middle interval of $P_{f,sec}$, e.g., from 0.006 ($\beta_{sec} = 2.51$) to 0.016 ($\beta_{sec} = 2.14$). This interval of $P_{f,sec}$ is called sensitive interval (SI). However, when the value of $P_{f,sec}$ is very small (3.17×10^{-5}–6.00×10^{-3}) or very large (0.016–0.159), the $P_{f,sys}$ increases slowly. These two intervals are called insensitive intervals (II). If the section failure probability $P_{f,sec}$ lies in the SI, a minor change of $P_{f,sec}$ can trigger a considerable mutation in system safety, i.e., $P_{f,sys}$, suggesting that the section reliability evaluation requires higher precision than that when $P_{f,sec}$ is located out of SI.

3.3.2 Influence of the number of sections on system failure probability

Figure 7 shows the influence of section number n on the system failure probability $P_{f,sys}$, where the η_{acc} is fixed as 0.1% and n = 1000, 2000, 3000 are used for illustration. A larger n produces a steeper $P_{f,sys}$ curve in the middle range of $P_{f,sec}$, which leads to a narrower sensitive interval and wider insensitive intervals. That is, for a system with more components, the $P_{f,sys}$ is more sensitive to $P_{f,sec}$ located in SI and less sensitive to $P_{f,sec}$ located in II. Besides, for a given value of $P_{f,sec}$, the $P_{f,sys}$ with a larger n is not necessarily larger than that with a smaller n (see vertical dashed lines L1 and L2). Moreover, the same $P_{f,sys}$ may be observed even if different section numbers n are used (see the point of intersection), because of the different values of m that they have.

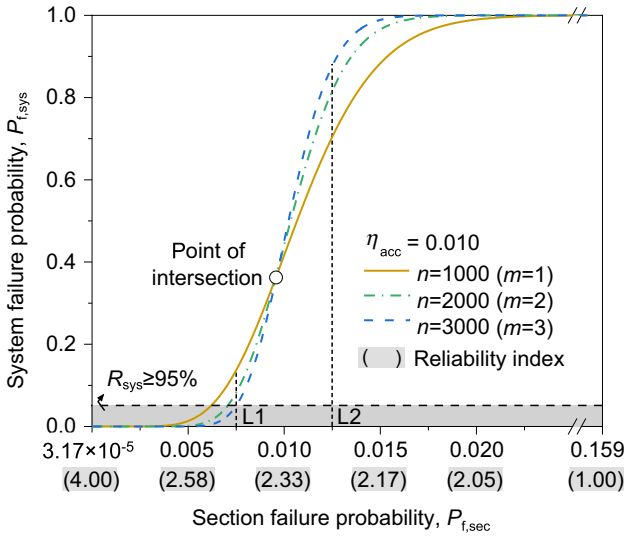

Fig. 7 Influence of n on $P_{f,sys}$

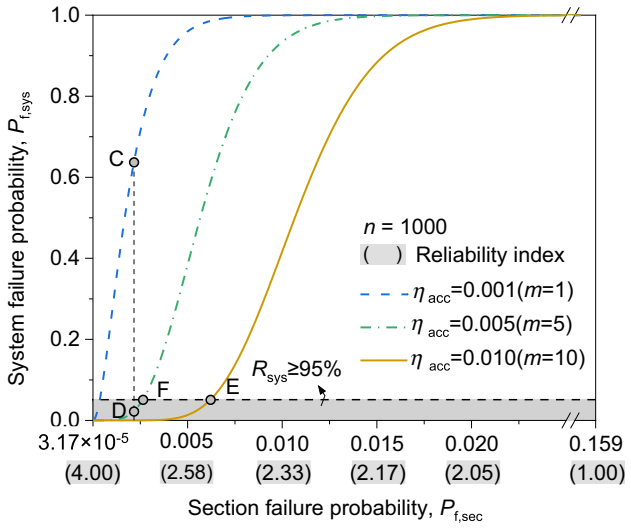

Fig. 8 Influence of η_{acc} on $P_{f,sys}$

3.3.3 Influence of acceptable failure ratio on system failure probability

Figure 8 shows the influence of the acceptable failure ratio η_{acc} on a system failure probability $P_{f,sys}$, where n is fixed at 1000. η_{acc} has a positive effect on the width of SI. That is, the larger the η_{acc} is, the less sensitive of $P_{f,sys}$ to $P_{f,sec}$ becomes. In addition, the $P_{f,sys}$ sharply decreases with the increase of η_{acc}. Taking $P_{f,sec} = 0.002$ for example, the $P_{f,sys}$ decreases from 64.3% (point C) to 2.4% (point D) when η_{acc} increases from 0.001 ($m = 1$) to 0.005 ($m = 5$). In other words, one has the confidence of 35.8% that m_{act} does not exceed 1, whereas one has the confidence of 97.6% that m_{act} does not exceed 5. Figure 8 also provides useful information for guiding the design of long subgrade slopes. For instance, if one hopes a subgrade slope has system reliability of 95% ($\beta_{sys} = 1.65$), the failure probability of each section is required to be less than 6.21×10^{-3} ($\beta_{sec} = 2.50$) when the acceptable failure ratio $\eta_{acc} = 0.010$ (point E). However, the $P_{f,sec}$ is required to be less than 2.64×10^{-3} ($\beta_{sec} = 2.80$) when the $\eta_{acc} = 0.005$ (point F). In other words, one can save lots of investment to improve the safety level of each section by slightly accepting more local instability events. When considering the economic criterion, the k-out-of-n system model provides an alternative approach to design the system reliability of subgrade slopes.

4 Case study

The spatial parameters of soil properties such as SOF are generally not required in the current design specifications of railway engineering, leading to a lack of such data in site investigation reports. Besides, subgrade slopes are not always continuous and soil properties are not always statistically homogeneous. To apply DDM at the current stage, the segmentation of long subgrade slopes and the calculation of sectional slope reliabilities need to be reasonably simplified. This section shows a possible way to apply DDM to a built high-speed railway project, in which only the point statistics of soil properties (i.e., mean and standard deviation) and slope geometries are accessible.

4.1 Problem description

The high-speed railway project to be assessed began in 2015 and was currently under construction at the time of writing this article. The total length of the railway line is 211 km with mileage from K5 + 000 to K216 + 000, of which the total length of subgrades is around 206 km, including 46.91 km of cuttings, 13.18 km of embankments, and 5.91 km to be constructed. The rail line is located in elevated portions of the temperate zone, with elevation ranging from 1200 to 2000 m. The region along the route has a semi-arid climate featuring dry and warm to hot summers and cold winters. Due to such topography and climate conditions, water infiltration and seepage rarely happen, and the likelihood of rainfall-induced slope instability events is extremely low.

In the site investigation report, three types of slopes were not considered since they have little effect on railway safety, including (1) a slope height less than 2 m, (2) a slope gradient less than 1:3, and (3) a distance larger than 3 m between the toe of cutting slopes and the ditch of the engineered structure. Table 3 shows the number and geometries of 2345 surveyed cross-sectional soil slopes. Rock slopes

Table 3 Mileage and the number of cross-sections

Slope type	Mileage	Number of cross-sections	Gradient range	Height range (m)
Embankment	K5 + 000–K15 + 000	135	1:2–1:3	2–16.62
	K15 + 000–K19 + 721	51	1:2–1:3	2–16.65
	K19 + 721–K25 + 000	91	1:1.83–1:3	2–23.80
	K25 + 000–K40 + 000	69	1:1.67–1:3	2–12.46
	K40 + 000–K51 + 000	85	1:1.67–1:3	2–8.27
	K51 + 000–K62 + 000	182	1:1.5–1:3	2–11.17
	K62 + 000–K102 + 300	N.A.	N.A.	N.A.
	K102 + 300–K118 + 250	118	1:2–1:3	2–7.99
	K118 + 250–K130 + 000	82	1:1.85–1:3	2–14.54
	K130 + 000–K140 + 000	111	1:1.6–1:3	2–9.14
	K140 + 000–K155 + 000	268	1:1.8–1:3	2–7.28
	K155 + 000–K165 + 560	230	1:2–1:3	2–8.55
	K165 + 560–K175 + 000	150	1:1.92–1:3	2–5.14
	K175 + 000–K185 + 000	55	1:1.8–1:3	2–5.25
	K185 + 000–K195 + 000	200	1:1.92–1:3	2–4.23
	K195 + 000–K205 + 000	132	1:1.8–1:3	2–8.65
	K205 + 000–K216 + 000	158	1:1.8–1:3	2–9.60
Cutting	Soil slope	228	1:0.6–1:2.8	2–15.45
	Rock slope	346	1:0.35–1:6.88	2–30.95
In total	Soil slope	2345	N.A.	N.A.
	Rock slope	346	N.A.	N.A.

N.A. stands for not available

are not considered in the current system reliability evaluation of subgrade slopes. The point statistics of soil strength parameters are listed in Table 4, including the mean (μ_c) and standard deviation (σ_c) of cohesion, the mean (μ_φ) and standard deviation (σ_φ) of friction angle, and the coefficient of variation of cohesion (V_c) and friction angle (V_φ). The unit weight γ of soil embankments is approximately 19 kN/m^3, and γ = 20–22 kN/m^3 for soil cuttings. The variability

Table 4 Mileage and the statistics of soil strength parameters

Mileage	μ_c (kPa)	μ_φ (°)	σ_c (kPa)	σ_φ (°)	V_c	V_φ
K5 + 000–K15 + 000	16.52	40.42	10.17	3.02	0.62	0.07
K15 + 000–K19 + 721	14.75	40.04	6.74	4.51	0.46	0.11
K19 + 721–K25 + 000	17.71	41.81	7.72	3.21	0.44	0.08
K25 + 000–K40 + 000	22.53	44.33	7.93	2.07	0.35	0.05
K40 + 000–K51 + 000	23.87	37.93	6.31	3.68	0.26	0.10
K51 + 000–K62 + 000	21.29	43.88	6.37	4.68	0.30	0.11
K62 + 000–K102 + 300	N.A.	N.A.	N.A.	N.A.	N.A.	N.A.
K102 + 300–K118 + 250	20.94	43.53	9.58	3.43	0.46	0.08
K118 + 250–K130 + 000	25.22	44.90	7.14	1.78	0.28	0.04
K130 + 000–K140 + 000	17.44	34.03	7.95	2.57	0.46	0.08
K140 + 000–K155 + 000	14.08	39.74	7.22	3.50	0.51	0.09
K155 + 000–K165 + 560	12.49	37.3	5.74	2.60	0.46	0.07
K165 + 560–K175 + 000	10.50	38.31	5.19	2.12	0.49	0.06
K175 + 000–K185 + 000	15.37	44.57	7.23	4.00	0.47	0.09
K185 + 000–K195 + 000	9.55	42.20	7.09	4.51	0.74	0.11
K195 + 000–K205 + 000	4.13	37.66	3.33	1.99	0.81	0.05
K205 + 000–K216 + 000	4.63	37.61	3.76	1.49	0.81	0.04

N.A. stands for not available

of γ is rationally neglected. The site investigation was carried out between 2015 and 2018. For soil samples collected in embankments, direct shear tests were performed on these samples to obtain their strength properties. Dynamic cone penetration testing was used on-site to evaluate the mechanical properties of soil samples in cut sections [30], and the original data were converted to cohesion and friction angles [31] to facilitate the probabilistic analysis of soil slope stability. During the investigation, local instabilities of two distant cut slopes were reported.

4.2 Segmentation of long subgrade slope

There are two stages to divide the subgrade slope into multiple sections. In the first stage, the subgrade is divided into many segments in the following principles: (1) the boundary between subgrade slope and structure, such as bridge, (2) a change in the type of slope, i.e., cutting and embankment, (3) an apparent change of slope height, i.e., greater than 1 m, and (4) an apparent change in the statistics of strength parameters such that they can no longer be regarded as statistically homogeneous. In the second stage, continuous subgrade slope segments composed of statistically homogeneous soils, they are further divided into multiple sections as per Sect. 2. Nevertheless, the SOF of soil properties is not provided in the survey report, and the number of sections cannot be directly computed.

Based on the work of Hicks and Li [13], the θ_h of soil properties typically ranges from 10 to 100 m, and L_{sec} is around 3.5 to 1.5 folds of θ_h as θ_h increases from 12 to 100 m. That is, L_{sec} varies from 35 to 150 m when θ_h is unknown. For slopes with different parameters, these ratios may change. To divide continuous long subgrade slopes into multiple sections, a simplified yet practical DDM is proposed herein. The value of 100 m is adopted as the empirical value of L_{sec}. For a segment, the residual length less than 100 m will be ignored. Discretely distributed subgrade segments shorter than 100 m are regarded as individual sections. In total, there are 997 slope sections. For comparison, $L_{sec} = 50$ m is also analyzed. The corresponding total number of slope sections is 1980.

4.3 Computation of sectional slope reliability

For the reliability analysis of long soil slopes, Vanmarcke [15] proposed an analytical method using local average theory in which sliding mass is assumed to be a cylinder cut by two vertical planes. Zhang et al. [32] improved the Vanmarcke method by changing vertical planes to ellipsoidal surfaces which is more in line with reality. They can also be analyzed using RFEM [33]. However, all the above methods require the horizontal and vertical scale of fluctuations, which are not available in most current investigation reports. Based on slope geometries and the point statistics of soil properties, only the reliability analysis of cross-sectional slope can be carried out.

Whether or not considering the spatial variability of soil parameters, the reliability obtained by three-dimensional probabilistic analysis (R_{sec}) is generally greater than that of cross-sectional analysis (R_{cs}) due to end effect [15, 32]. The end effect means that the resisting moment provided by two end parts of a three-dimensional sliding mass is larger than the driving moment provided by it. That is, using two-dimensional slope reliability analysis results instead of three-dimensional slope reliability analysis results is on the conservative side. In this case study, the reliability of slope sections will be substituted by that of cross-sections taken from them, i.e., letting $R_{sec} = R_{cs}$. The histograms of the reliability index (β_{sec}) of slope sections are shown in Fig. 9. In the two situations, the mean of β_{sec} is 4.49, and the mean and standard deviation (s.d.) of β_{sec} are almost the same; the slope with $\beta_{sec} > 2$ accounts for more than 99.5%, and the slope with $\beta_{sec} > 3$ accounts for more than 97.5%. The number of slopes with $\beta_{sec} < 2$ for the two situations is only 5 and 9, respectively. For most engineered slopes, $\beta = 2$–3 is usually thought to be large enough to ensure stability, corresponding to a failure probability of 2.3%–0.13%.

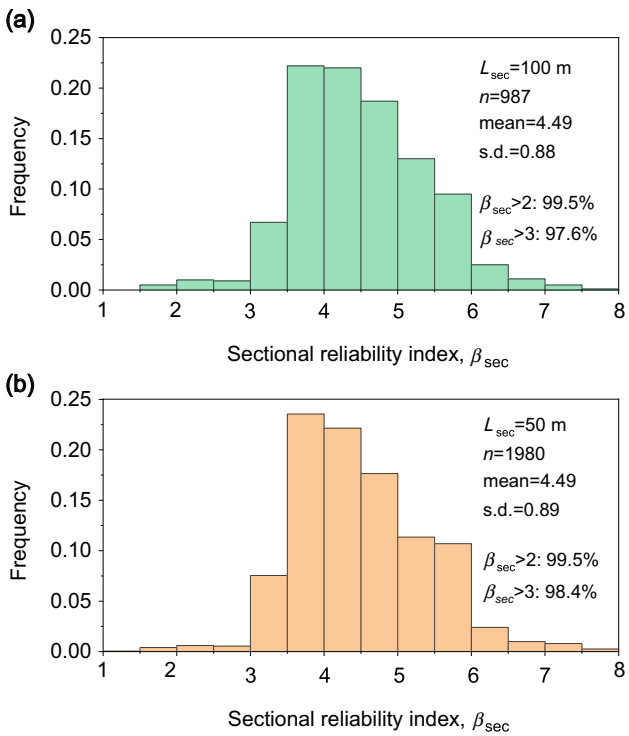

Fig. 9 Histogram of β_{sec}: **a** $L_{sec} = 100$ m; **b** $L_{sec} = 50$ m

4.4 Evaluation of system reliability

Figure 10 shows the occurrence probability P versus the actual number of failure sections m_{act}, which changes from 0 to 5. For the situation of L_{sec} = 100 m, the probability P of the event that no local instability will occur is 63%, i.e., m_{act} = 0, and P = 29% for the event that m_{act} = 1. P decreases nonlinearly with increasing m_{act}. When the actual number of failure sections reaches 4, the occurrence probability is only 8.5×10^{-3}. That is, the most possible result is that the actual number of failure sections equals zero. The probability of the event that the total number of failure sections is no greater than 2 reaches up to 98.30%. Thus, if the acceptable number of failure sections m is 2, the system failure probability will be $P_{f,sys}$ = 1.70%. For the situation of L_{sec} = 50 m, the decreasing law of P is also applicable. The probability of the event that the total number of failure sections is no greater than 2 reaches up to 97.00%.

Figure 11 shows the curve of system failure probability $P_{f,sys}$ versus the acceptable number of failure sections m, where $P_{f,sys}$ decreases sharply with the increase of m from 0 to 5. In the Chinese code for risk management of railway construction engineering [34], the occurrence probability of an event is divided into five categories, corresponding to events with different frequencies, including frequently ($P \geq 0.3$), occasionally ($0.03 \leq P < 0.3$), seldom ($0.003 \leq P < 0.03$), rarely ($0.0003 \leq P < 0.003$), and almost never ($P < 0.0003$), as displayed in Fig. 11. For the situation of L_{sec} = 100 m, the acceptable number of failure sections varying from 0 to 5 can be frequently, occasionally, seldom, rarely, and almost never exceeded by actual values m_{act}. The system reliability level can be described as having a 36.6% confidence that the actual number of failure sections is greater than 0, or having a 0.90% confidence that the actual number of failure sections is greater than 2, etc. The full data is listed in Table 5. Based on Figs. 9 and 11, although most cross-sectional slope reliability indices are larger than 3, there is still a considerable probability to encounter several local instability events along the railway line. This corroborates the length effect in the system reliability analysis of long side slopes. For the situation of L_{sec} = 50 m, the $P_{f,sys}$ is always larger than that of the situation of L_{sec} = 100 m, because the number of components in the former system is twice the latter one.

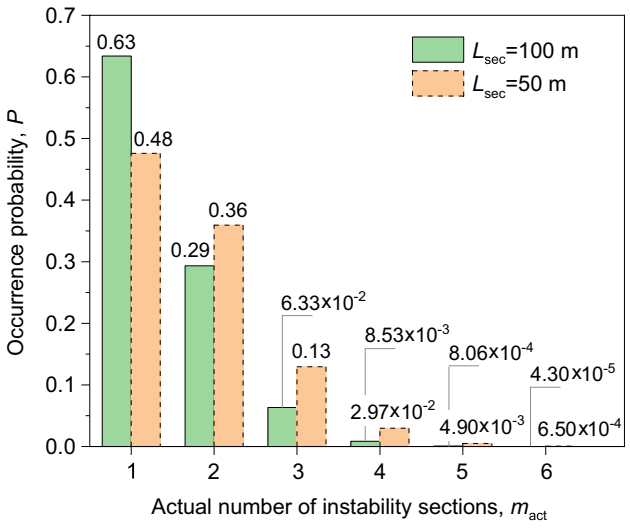

Fig. 10 Histogram of occurrence probability

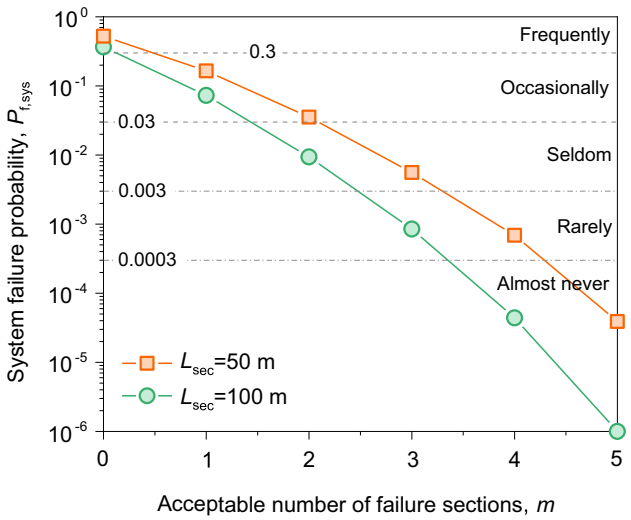

Fig. 11 Results of system failure probability

There are two aspects of simplifications when applying DDM to the real subgrade slope system lacking spatial data. One is the segmentation of subgrade slopes based on empirical L_{sec}, and the other is using R_{cs} to substitute R_{sec} For the former simplification, the prediction of system reliability may be conservative ononconservative depending on the magnitude of L_{sec} (e.g., 50 m) relative to the actual section length determined by rigorous approaches. Based on the case study, when making L_{sec} = 50 and 100 m respectively, the difference between $P_{f,sys}$ rapidly increases with increasing m (see Fig. 10). That is, the determination of L_{sec} has a

Table 5 Calculation results of system failure probability

m	$P_{f,sys}$	
	L_{sec} = 100 m	L_{sec} = 50 m
0	0.366020	0.524180
1	0.072730	0.164840
2	0.009380	0.035330
3	0.000850	0.005590
4	0.000044	0.000689
5	0.000001	0.000039

considerable impact on prediction results, and an unreasonable value of L_{sec} may lead to wrong outcomes. The latter simplification is conservative since R_{sec} is always greater than R_{cs}. Based on Zhang et al. [32], the ratio R_{sec}/R_{cs} decreases with the increase of the length of sliding mass or the horizontal SOFs of shear strength parameters. For slopes with typical geometry and soil parameters, the ratio mostly ranges from 1 to 2.

For subgrade slopes that lack essential spatial data, the computation of system reliability on the basis of empirical L_{sec} and R_{cs} provides decision-makers helpful additional information to get as comprehensive a picture of long subgrade slope systems as possible, although the two simplifying measures bring uncertainties to the prediction of system safety level. Actually, various methods have been developed to characterize this parameter from soil data, particularly CPT measurements [19]. Thus, to assess the system safety of long subgrade slopes using DDM, one of the greatest challenges lies in incorporating the survey of SOF into site investigation specifications. Another major challenge stems from the specificity of soil properties at different sites, which is a distinctive and fundamental feature of geotechnical engineering practice. To overcome this limitation, the establishment of a global database of SOFs will be a meaningful work direction [35].

5 Concluding remarks

This paper develops a DDM method to evaluate the system reliability performance of long subgrade slopes. DDM is an improvement of the VNK method in three aspects. First, long subgrade slopes are segmented into multiple adjacent sections based on the number of potential local instabilities predicted by the random finite element method. Second, two indicators are adopted to describe the system reliability performance, namely the acceptable number of failure sections m and the system reliability R_{sys}. The former characterizes the designer's expectation of system safety, and the latter expresses the confidence that m will not be exceeded. Third, the k-out-of-n system model with redundancy features is introduced to establish the relationship between the tolerance threshold m and the system reliability R_{sys}.

Parametric analyses are conducted to investigate the influence of impact factors on system reliability. The total number of slope sections n is negatively related to the horizontal SOF of soil properties and positively related to the length of subgrade slopes. R_{sys} decreases with increasing n, decreasing m, or decreasing reliability of slope sections R_{sec}. Subgrade slopes with larger length or weaker soil strength face a higher risk to encounter more local instabilities, and there may still be a considerable possibility to encounter local instabilities even if all sections have high reliability. When analyzing or designing the stability of subgrade slopes, system reliability should be given sufficient attention in addition to the traditional cross-sectional reliability.

A case study is provided to show the application of DDM when lacking spatial data of soil proprieties. The DDM is simplified in two aspects. First, subgrade slopes are segmented into many sections based on the empirical length of slope sections L_{sec}. Second, the reliability of sections R_{sec} is substituted by that of cross-sections R_{cs} taken from them. The first simplifying measures may lead to conservative or unconservative results, and the second will make the system reliability analysis results conservative. Nevertheless, by cautiously estimating the lower and upper values of L_{sec}, one can roughly evaluate the bounds of system reliability using the simplified DDM. It is highly recommended that the spatial data of soil properties be determined in future site investigations.

In many cases, subgrades, bridges, and tunnels together form the foundation of a railroad. In addition to subgrade slopes, there are usually a large number of natural slopes along the line, and their instability will also have a great impact on rigid structures as well as transition sections [36, 37]. In a broad sense, all slopes along a rail line can be regarded as the k-out-of-n system. By analyzing the reliability of this system, the overall landslide risk of a line can be assessed.

Acknowledgements The work was supported by the National Natural Science Foundation of China (Nos. 52078435 and 51878560). Professor Kok-Kwang Phoon and Dr. Chong Tang from National University of Singapore and Dr. Jifeng Lian from Xihua University are greatly appreciated for their useful suggestions in the process of preparing this manuscript. The first author would greatly like to thank the financial support from the open research fund of MOE Key Laboratory of High-Speed Railway Engineering.

References

1. Nguyen TT, Indraratna B (2022) Rail track degradation under mud pumping evaluated through site and laboratory investigations. Int J Rail Transp 10(1):44–71

2. Lin Z, Niu F, Li X et al (2018) Characteristics and controlling factors of frost heave in high-speed railway subgrade, Northwest China. Cold Reg Sci Technol 153:33–44
3. Wikipedia (2021) Ingenheim derailment https://en.wikipedia.org/wiki/Ingenheim_derailment. Accessed 24 Feb 2022
4. Zhang LL, Zhang J, Zhang LM et al (2011) Stability analysis of rainfallinduced slope failure: a review. Proc Inst Civ Eng Geotech Eng 164(5):299–316
5. Hicks MA, Spencer WA (2010) Influence of heterogeneity on the reliability and failure of a long 3D slope. Comput Geotech 37(7–8):948–955
6. Duncan JM, Wright SG, Brandon TL (2014) Soil Strength and Slope Stability, 2nd edn. John Wiley & Sons, Hoboken, NJ, USA
7. Fellenius W (1936) Calculation of stability of earth dam. In: Proceedings of the Second Congress of Large Dams, Washington, DC, vol 4, pp 445–462
8. Cho SE (2013) First-order reliability analysis of slope considering multiple failure modes. Eng Geol 154:98–105
9. Low BK, Tang WH (2007) Efficient spreadsheet algorithm for first-order reliability method. J Eng Mech 133(12):1378–1387
10. Christian JT, Ladd CC, Baecher GB (1994) Reliability applied to slope stability analysis. J Geotech Eng 120(12):2180–2207
11. Griffiths DV, Fenton GA (2004) Probabilistic slope stability analysis by finite elements. J Geotech Geoenviron Eng 130(5):507–518
12. Reale C, Xue J, Pan Z et al (2015) Deterministic and probabilistic multi-modal analysis of slope stability. Comput Geotech 66:172–179
13. Hicks MA, Li YJ (2018) Influence of length effect on embankment slope reliability in 3D. Int J Numer Anal Methods Geomech 42(7):891–915
14. Vanmarcke E (2014) Multi-hazard risk assessment of civil infrastructure systems with a focus on long linear structures such as levees. In: Liu XL, Ang AH-S (eds) Sustainable development of critical infrastructure. International Conference on Sustainable Development of Critical Infrastructure, May 16–18, 2014, Shanghai, China. Reston, VA, USA: American Society of Civil Engineers, 2014: 37–56
15. Vanmarcke E (1977) Reliability of earth slopes. J Geotech Eng Div 103(11):1247–1265
16. Vanmarcke E (2010) Random fields: analysis and synthesis (revised and expanded new edition). World Scientific, Singapore. https://doi.org/10.1142/5807
17. El-Ramly H, Morgenstern NR, Cruden DM (2003) Probabilistic stability analysis of a tailings dyke on presheared clay shale. Can Geotech J 40(1):192–208
18. Phoon KK, Kulhawy FH (1999) Characterization of geotechnical variability. Can Geotech J 36(4):612–624
19. Cami B, Javankhoshdel S, Asce AM et al (2020) Scale of fluctuation for spatially varying soils: estimation methods and values. ASCE ASME J Risk Uncertain Eng Syst Part A Civ Eng 6(4):03120002
20. Phoon KK, Retief JV (2016) Reliability of geotechnical structures in ISO2394. CRC Press/Balkema, Leiden, Netherlands
21. VPO (2012) Flood risk in the netherlands: the method in brief. Utrecht, Netherlands: VNK Project Office
22. VPO (2014) The national flood risk analysis for the Netherlands: Final report. Utrecht, Netherlands: VNK Project Office
23. Jongejan RB, Calle EOF (2013) Calibrating semi-probabilistic safety assessments rules for flood defences. Georisk Assess Manag Risk Eng Syst Geohazards 7(2):88–98
24. Melchers RE, Beck AT (2017) Structural reliability analysis and prediction, 3rd edn. John Wiley Sons, Hoboken, NJ, USA. https://doi.org/10.1002/9781119266105
25. Barlow RE, Proschan F (1965) Mathematical theory of reliability. John Wiley Sons, New York, NY, USA. https://doi.org/10.1137/1.9781611971194
26. Salgado R, Kim D (2014) Reliability analysis of load and resistance factor design of slopes. J Geotech Geoenviron Eng 140(1):57–73
27. Ching JY, Hu YG, Yang ZY et al (2011) Reliability-based design for allowable bearing capacity of footings on rock masses by considering angle of distortion. Int J Rock Mech Min Sci 48(5):728–740
28. ISO (2015) ISO 2394 General principles on reliability of structures. Geneva, Switzerland: International Organization for Standardization
29. Orr TLL (2019) Honing safety and reliability aspects for the second generation of Eurocode 7. Georisk Assess Manag Risk Eng Syst Geohazards 13(3):205–213
30. Salgado R, Yoon S (2003) Dynamic cone penetration test (DCPT) for subgrade assessment. Indiana: Purdue University, West Lafayette
31. USBR (2002) Engineering geology field manual, 2nd edn. US Department of the Interior Bureau of Reclamation, Washington, DC
32. Zhang W, Luo Q, Jiang L et al (2021) Improved Vanmarcke's analytical model for 3D slope reliability analysis. Comput Geotech 134:104106
33. Xiao T, Li DQ, Cao ZJ et al (2016) Three-dimensional slope reliability and risk assessment using auxiliary random finite element method. Comput Geotech 79:146–158
34. Office of China Railway (2015) Technical code for risk management of railway construction engineering (Q/CR 9006-2014). China Railway Publishing House, Beijing (**in Chinese**)
35. Ching JY, Phoon KK, Khan Z et al (2020) Role of municipal database in constructing site-specific multivariate probability distribution. Comput Geotech 124:103623
36. Meng XM, Qi TJ, Zhao Y et al (2021) Deformation of the Zhangjiazhuang high-speed railway tunnel: an analysis of causal mechanisms using geomorphological surveys and D-InSAR monitoring. J Mt Sci 18(7):1920–1936
37. Zhou S, Tian Z, Di H et al (2020) Investigation of a loess-mudstone landslide and the induced structural damage in a high-speed railway tunnel. Bull Eng Geol Environ 79(5):2201–2212